Proceedings of the 35th European Safety and Reliability & the 33rd Society for Risk Analysis Europe Conference
Edited by Eirik Bjorheim Abrahamsen, Terje Aven, Frederic Bouder, Roger Flage, Marja Ylönen
 Published by Research Publishing, Singapore.
doi: 10.3850/978-981-94-3281-3_ESREL-SRA-E2025-P2114-cd

A hybrid method for future capacity and RUL prediction of lithium-ion batteries considering capacity regeneration

Guisong Wang

School of Reliability and Systems Engineering, Beihang University, Beijing, China. E-mail: wgskl@buaa.edu.cn

Yunxia Chen

School of Reliability and Systems Engineering, Beihang University, Beijing, China. E-mail: chenyunxia@buaa.edu.cn

Jie Liu

School of Reliability and Systems Engineering, Beihang University, Beijing, China. E-mail: Liujie805@buaa.edu.cn

Accurate prediction of remaining useful life (RUL) is critical to the reliability and safety of lithium-ion batteries. However, challenges frequently arise when using the measured data for RUL prediction, such as degradation data being significantly influenced by noise and difficulties in estimating uncertainty induced by capacity regeneration. To address this issue, a hybrid prediction method to predict battery future capacity and RUL is proposed by combining the adaptive variational modal decomposition (AVMD), permutation entropy (PE), long short-term memory (LSTM) network and Bayesian neural network (BNN). Specifically, the AVMD algorithm is employed to decompose the battery capacity data into the aging trend sequence at low frequencies and the noise and capacity regeneration sequences at high frequencies. AVMD adaptively optimizes the number of decomposition stages and balancing parameters through kernel estimation for mutual information and the relative energy density gradient as the objective function. PE is utilized to adaptively filter the high-frequency and low-frequency sequences while eliminating the noise sequence. The prediction models based on LSTM and BNN are then respectively developed to forecast the aging trend sequence and capacity regeneration sequence. The proposed hybrid method demonstrates broad applicability and minimal prediction error as verified by the application on lithium-ion battery dataset.
Keywords: Lithium-ion batteries, Remaining useful life, Adaptive variational modal decomposition, Permutation entropy, Long short-term memory network, Bayesian neural network.

1. Introduction

Lithium-ion batteries are widely used as the main power supply components in various systems such as electronic devices and spacecraft, due to their long cycle life, high energy density, and no memory effect. However, in practical applications, the performance of the battery continuously degrades with repeated charging and discharging due to the presence of side reactions. It is generally believed that when the capacity drops below 80% of the initial capacity, the device battery will no longer meet the normal usage requirements and must be replaced (Ge et al., 2021; Li et al., 2019; Song et al., 2023).

PHM of lithium-ion batteries enables users to make maintenance decisions in advance to prevent losses caused by unexpected failures. Remaining useful life (RUL) prediction is a core issue of PHM (Cong et al., 2020; Waag et al., 2014). To predict the RUL of a battery, it is necessary to establish a battery aging model that can capture the degradation characteristics of lithium-ion batteries and predict the degradation characteristics based on measured data as input. However, the collected data are often non-stationary and are greatly affected by noise terms, so it is a huge challenge to establish a model that can simultaneously capture the long-term dependence of capacity and the uncertainty caused by fluctuations such as capacity regeneration.

Existing RUL prediction methods are mainly divided into model-based approaches and data-driven approaches. Model-based methods generally use mathematical representations to characterize battery capacity degradation (Barré et al., 2013), such as electrochemical models (Yang et al., 2017) and equivalent circuit models (Guha et al., 2017) and are combined with filtering techniques (Chang et al., 2017; Lyu et al., 2017) to predict the RUL of batteries. This approach heavily relies on expert knowledge about battery degradation. Moreover, observer techniques such as particle filtering are prone to particle depletion problems, leading to inaccurate RUL predictions (K. Liu et al., 2021).

Compared with model-based methods, data-driven methods rely solely on historical

degradation data without the need for explicit mathematical models to describe the battery degradation process, and therefore have been widely applied. An increasing number of studies apply machine learning techniques to predict the RUL of batteries, including neuro-fuzzy networks (NF) (Razavi-Far et al., 2009), Gaussian process regression (GPR) (Richardson et al., 2017), relevance vector machine (RVM) (C. Zhang et al., 2017), and backpropagation neural networks (BP) (Wu et al., 2016), which map feature data to RUL through the constructed black-box models. Liu et al. (J. Liu et al., 2012) proposed a hybrid model-data-driven method, using the data-driven part to predict the future measurements of the battery. However, these methods directly use the measured capacity data for research, and noisy battery aging data often reduces the performance of the prediction models. The VMD algorithm is an adaptive mode decomposition and signal processing method, which adaptively decomposes the signal into a series of intrinsic mode functions (IMFs) (Jiang et al., 2022). The decomposition effect of the VMD algorithm is significantly affected by the decomposition level and balance coefficient, which are usually preset values. In the existing literature, research on the joint optimization of the decomposition level and balance coefficient parameters is still insufficient.

In conclusion, this paper proposes a hybrid method for predicting the future capacity and RUL of lithium-ion batteries considering capacity regeneration. The adaptive variational mode decomposition (AVMD) overcomes the problem of the traditional VMD method, where the decomposition effect is significantly affected by the decomposition level k and the balance parameter α, achieving more accurate mode decomposition. The permutation entropy (PE) method automatically excludes noise sequences containing less effective information, eliminating the influence of noise and improving the accuracy of RUL prediction. LSTM models capable of capturing the long-term dependence of battery capacity decay and BNN models capable of capturing the uncertainty caused by capacity regeneration are established, respectively. Finally, by comparing with traditional data-driven methods, the effectiveness and superiority of our method are verified.

2. Methodology

In this section, a hybrid method for predicting the future capacity and RUL of batteries is introduced. Traditional methods face issues such as significant noise interference, difficulty in capturing long-term dependencies in time series, and the presence of capacity regeneration phenomena in the original data. To address these issues, the data-driven method proposed in this paper consists of three main parts: the AVMD method for accurately decomposing the original capacity data set, the LSTM sub-model capable of capturing long-term dependencies, and the BNN sub-model capable of generating prediction result uncertainties. Fig.1 illustrates the framework of the proposed method.

2.1. *Fundamentals of the VMD algorithm*

Variational Mode Decomposition (VMD) (Ge et al., 2021) is an adaptive method for variational mode decomposition and signal processing. It overcomes the disadvantages of mode mixing and boundary effects present in the Empirical Mode Decomposition (EMD) method. The steps of the VMD algorithm can be briefly described as follows:

(1) Choose the decomposition modes count k and balance parameter α. Initialize the modes $mod_k(t)(k = 1, \cdots, K)$.

(2) Combine the analytic signal with the complex exponential term of the estimated central frequency to obtain the mixed signal. Translate the spectrum of the mixed signal to align with the estimated central frequency ω_k:

$$\min_{\{mod_k\},\{\omega_k\}} \left\{ \sum_{k=1}^{K} \left\| \partial_t \left[\left(\delta(t) + \frac{i}{\pi t} \right) * mod_k(t) \right] e^{-i\omega_k t} \right\|_2^2 \right\} \quad (1)$$

where $||\ ||_2$ represents the L2-norm, $*$ is the convolution operator, $i = \sqrt{-1}$, and δ is the Dirac distribution.

(3) Eq.(1) can be transformed into an unconstrained equation as in (Ge et al., 2021) through quadratic penalty terms and Lagrange multipliers.

2.2. *The proposed AVMD algorithm*

The proposed AVMD method uses the kernel

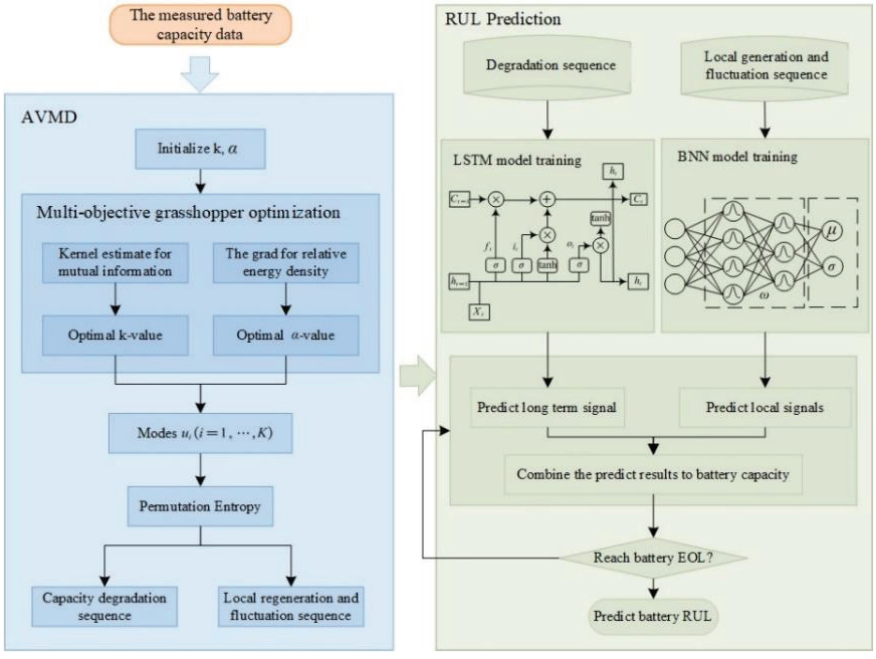

Fig. 1. Framework for predicting future capacity and RUL based on the proposed data-driven model.

estimation of mutual information and the gradient of relative energy density as constraints, with the decomposition series k and the balance parameter α as optimization targets. It achieves parameter optimization through the Multi-Objective Grasshopper Optimization Algorithm (MOGOA) (Mirjalili et al., 2018). The kernel estimation of mutual information (Kumar et al., 2021) is used to determine the decomposition series k. The selection of the balance parameter has always been a challenge in VMD, and the relative energy density (Jiang et al., 2019) can characterize the bandwidth of the decomposed modes.

The calculation process of kernel estimation of mutual information is outlined in (Kumar et al., 2021). The KEMI is:

$$\mathrm{KEMI}(f_i; l_i) = \frac{1}{N}\sum_i log\,\frac{p(f_i, l_i)}{p(f_i)p(l_i)} \tag{2}$$

To prevent mode mixing, the mutual information among modes should be reduced, and to avert information loss during decomposition, the sum of mutual information between all modes and the original signal need to be maximized. Consequently, a function is proposed to characterize the ratio of the sum of mutual information among modes to the sum of mutual information between the original signal and the modes. This function can be described as:

$$\mathrm{KEMI}_{\mathrm{fit}} = \frac{\sum_{k=1}^{K-1} KEMI(mod(k), mod(k+1))}{\sum_{k=1}^{K} KEMI(mod(k), f)} \tag{3}$$

The balance parameter α is used to balance the relationship between data fidelity and the bandwidth constraint of the components. A broad bandwidth may incorporate considerable noise into the modes, whereas a narrow bandwidth may exclude some valuable information from the modes. There is limited research on the selection of the balance parameter, making it difficult to specify an exact balance parameter coefficient before VMD. Indicators based on kurtosis and envelope are widely used for parameter optimization in the mode decomposition of mechanical vibration signals but are not suitable for the VMD of battery degradation data. Reference (Jiang et al., 2019) defines an indicator that accurately assesses the bandwidth characteristics, the energy density (ED), which reflects the frequency domain coverage of the corresponding mode, and the relative energy density (RED), indicating the proportional

bandwidth of the decomposed mode. As the RED increases, the wider the bandwidth of the decomposed mode; the bandwidth is co-regulated by the quantity of decomposition modes and the balance parameter. The RED is:

$$E(\alpha, K) = \frac{(\sum_{k=1}^{K} E_k(\alpha, K))/K}{\sum_{i=1}^{N}[x(i)]^2/N} \quad (4)$$

E_k represents the ED of each mode $u_k(j)(j = 1,2,\dots,N)$:

$$E_k(\alpha, K) = \frac{1}{N}\sum_{j=1}^{N}[u_k(j)]^2 \quad (5)$$

Essentially, a larger RED corresponds to a broader bandwidth of $u_k(j)(j = 1,2,\dots,N)$. As shown in Fig.2, both the decomposition mode number and the balance parameter jointly affect the RED. When the balance parameter is small, a slight change in the balance parameter can cause significant fluctuations in the mode bandwidth, and an excessively large bandwidth may cause some components to encompass other components. We select the optimal balance parameter when the gradient of the RED is close to 0, at which point the RED is essentially unaffected by the balance parameter. This method ensures that no component encompasses another. When the gradient of RED is approximately equal to 0, in the flat region shown in Fig.2, indicating the optimal balance parameter coefficient:

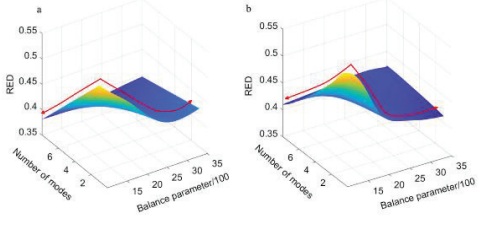

Fig.2 The relationship betwsseen the RED and the number of modes and balance parameters.

$$\nabla\{E(\alpha_m, k_n)\} = \big(E(\alpha_{m+1}, k_n) - E(\alpha_m, k_n)\big)/(\alpha_{m+1} - \alpha_m) + \big(E(\alpha_m, k_{n+1}) - E(\alpha_m, k_n)\big)/(k_{n+1} - k_n) \quad (6)$$

$\nabla\{E(\alpha_m, k_n)\}$ represents the gradient of the RED, where k_n is the number of decomposition modes, and α_m is the balance parameter.

PE is a measure of the natural complexity of time series introduced by Bandt in (Bandt & Pompe, 2002). We normalize PE values to the range [0,1] using Eq.(7).

$$h(p) = H(p)/\ln(N - d + 1) \quad (7)$$

where $H(p)$ is the original PE value, N is the time series length, and d is the embedding dimension. PE reflects complexity: lower values (PE < 0.4) indicate regularity, while higher values (PE > 0.4) suggest randomness and noise. According to the literature (Jiang et al., 2019), the threshold for PE is suitably set at 0.4. When the PE value exceeds 0.4, it is considered that the decomposed component contains only a small amount of effective information or is pure noise. In this study, the PE threshold is set to 0.4.

2.4. *A Long short-term memory model*

LSTM, a type of Recurrent Neural Network (RNN), mitigates the exploding and vanishing gradients issues in time series sequences and is effective for long-term dependency predictions (Wang et al., 2023; Y. Zhang et al., 2018). The advantage of the LSTM framework lies in its ability to store or update key information through the manipulation of introduced gates. In the fig.3, a typical LSTM-based RNN model consists of three gates. The forget gate allows for the deletion of information from the cell state c or the writing of information into the cell state c, the input gate determines whether the model can receive new state information, and the output gate decides which values of the cell state to output.

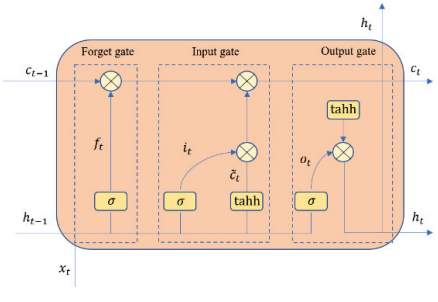

Fig.3 Structure of LSTM-based RNN model.

The decay values of capacity across different cycles are highly correlated. Therefore, LSTM will be used to capture the degradation trend sequences after AVMD.

2.5. *Bayesian neural network model*

Bayesian Neural Networks (BNNs) differ from conventional neural networks primarily in that their weight parameters are random variables following certain probability distributions, rather than fixed values.

Existing BNN models generally employ variational inference for training. A set of parameters controls the distribution $q(\omega|\theta)$ to approximate the true posterior $P(\omega|D)$. Typically, a Gaussian distribution $\theta = (u, \sigma)$ is used for this approxisamation. Each weight ω_i is sampled from a normal distribution (u_i, σ_i). The Kullback-Leibler (KL) divergence is used to measure the distance between two distributions:

$$\theta^* = \text{argmin}\text{KL}[q(\omega|\theta)||P(\omega|D)] \tag{8}$$

By further derivation, we obtain:

$$\theta^* = \text{argmin}E_{q(\omega|\theta)}[\log[\frac{q(\omega|\theta)}{P(D|\omega)P(\omega)}]] \tag{9}$$

$q(\omega|\theta)$ represents the distribution of the weight parameters; $P(D|\omega)$ represents the likelihood of the observed data given the weight parameters; $P(\omega)$ represents the prior of the weights. The inference problem of $P(\omega|D)$ is transformed into maximizing the Evidence Lower Bound (ELBO) problem:

$$\begin{aligned} &E_{q(\omega|\theta)}[\log q(\omega|\theta)] \\ &\quad - E_{q(\omega|\theta)}[\log q(Y|\omega, X)] \\ &\quad - E_{q(\omega|\theta)}[\log q(\omega)] \end{aligned} \tag{10}$$

Given a training dataset $\{x_i, y_i\}$, the Monte Carlo rule can be applied as per Eq.(10) to obtain:

$$\begin{aligned} &\sum_{i=1}^{m} \log q(\omega_i|\theta) - \sum_{i=1}^{m} \log q\left(y_j|\omega_i, x_j\right) \\ &\quad - \sum_{i=1}^{m} \log q(\omega_i) \end{aligned} \tag{11}$$

Using Eq.(11) as the loss function, the network structure is shown in Fig.4.

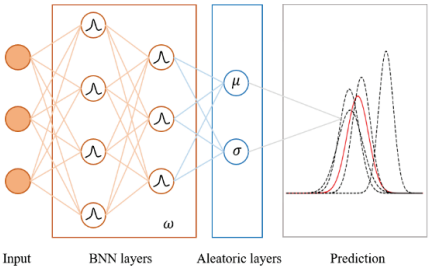

Fig.4 Structure of BNN model.

3. Case application and discussion

3.1. *Case data*

In this paper, the effectiveness and superiority of the proposed method is verified using experimental data from 20 commercial LCO/graphite batteries of various models from a lithium-ion battery manufacturer. These 20 batteries were cycled individually under a constant temperature condition of 25 ℃. Fig.5 shows the capacity degradation trajectory. Fig.6 takes batteries 14# and 15# as examples, there are obvious capacity regeneration phenomena during the degradation process.

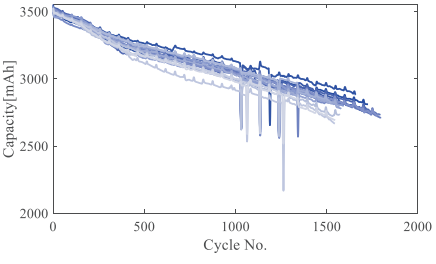

Fig.5 Capacity degradations versus cycle number.

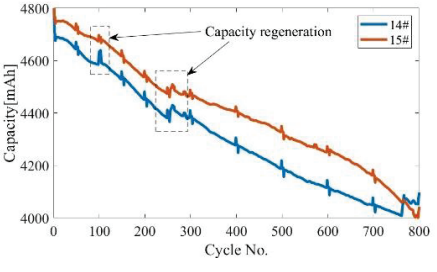

Fig.6 Capacity regenerations versus cycle number.

3.2. *Results and discussion*

The presence of PE values less than 0.4 for the decomposed components of the sample other than the degenerate sequences is found in only 5 samples. Fig.7 presents the final RUL prediction results based on the single LSTM model, single GPR model (For better graphical representation, the single GPR model discards the confidence ranges) and the hybrid method proposed in this paper. The lifetime of all samples is defined as the point at which they retain 80% of their initial capacity. Using half of the entire lifecycle data for observation, it is found that predictions based solely on LSTM or GPR are inferior to those based on the proposed method. Furthermore, apart from battery 12#, the prediction outcomes for the remaining batteries are notably satisfactory. To measure the accuracy of the proposed method, three evaluation metrics are introduced: Mean Absolute Error (MAE), Root Mean Square Error (RMSE), and Mean Absolute Percentage Error (MAPE). Their definitions are as follows:

$$MAE = \frac{1}{n-l}\sum_{i=l}^{n}\left|\hat{C}_i - C_i\right| \tag{12}$$

$$MAPE = \frac{1}{n-l}\sum_{i=l}^{n}\left|\frac{\hat{C}_i - C_i}{C_i}\right| \times 100\% \tag{13}$$

$$RMSE = \sqrt{\frac{1}{n-l}\sum_{i=l}^{n}\left(\hat{C}_i - C_i\right)^2} \tag{14}$$

here, $\hat{C}_i$ and C_i represent the predicted and actual capacities at the i-th cycle, respectively; n denotes the total number of cycles, and l indicates the starting cycle for prediction. Table 2 presents the statistical results of RUL prediction errors for the 5 test samples. Battery 1# has the highest prediction accuracy, while Battery 12# shows a more noticeable deviation in prediction. In Fig.7, the prediction uncertainty boundaries for all samples encompass the true predicted values. As the prediction step increases, the 95% confidence range will distribute in a wide region, indicating an increase in prediction uncertainty. This trend is attributed to the heightened uncertainty associated with long-term predictions.

Table 2 presents the prediction error results of the comparative experiments, where the proposed method significantly outperforms the standalone LSTM model. The RUL uncertainty bounds in Table 2 are defined by the confidence intervals associated with the battery EOL cycle. Among the multiple test samples, Battery #1 exhibits the widest confidence range. However, this value remains within an 8% range, suggesting that the model demonstrates robust extrapolation capabilities. Table 3 provides the final RUL prediction results for the 5 test samples based on the method proposed in this paper. The predicted RUL is relatively conservative compared to the actual RUL. The predicted RUL for batteries other than 12# is quite accurate; the RUL uncertainty bounds for batteries other than 12# effectively cover the actual RUL values.

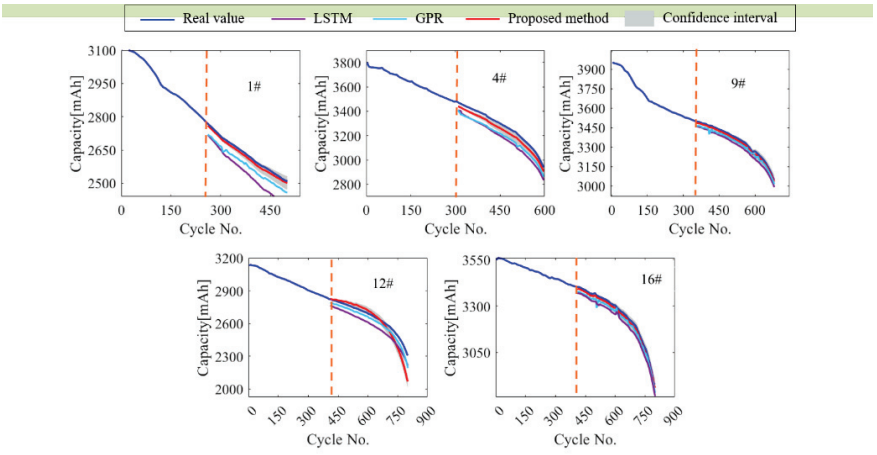

Fig.7 Predicted results of RUL for the proposed hybrid method and other two single methods.

Table 1. Prediction error for the five batteries.

Battery No.	LSTM			GPR			The proposed method		
	MAE	RMSE	MAPE	MAE	RMSE	MAPE	MAE	RMSE	MAPE
1#	72.25	42.66	2.68	42.22	24.46	1.56	11.08	6.44	0.41
4#	48.84	28.47	1.40	40.74	23.60	1.17	18.55	10.75	0.53
9#	68.61	40.80	2.26	45.42	28.63	1.49	21.34	12.63	0.70
12#	111.48	65.11	4.57	55.20	34.15	2.30	64.09	58.01	2.81
16#	66.65	39.58	2.15	40.94	25.23	1.30	19.33	11.40	0.62

Table 2. Performance of RUL predictions.

Battery No.	Actual EOL	Actual RUL	Predicted RUL	RUL uncertainty
1#	501	251	236	[220,259]
4#	594	297	291	[294,313]
9#	681	341	338	[328,356]
12#	801	401	364	[352,377]
16#	802	401	394	[388,402]

While acknowledging the effectiveness of the proposed method, it is important to note that AVMD represents a computationally intensive step. Specifically, the use of a MOGOA to iteratively compute kernel estimates for mutual information among decomposed modes and the gradients of relative energy densities significantly contributes to its time-consuming nature. This computational burden is primarily due to the need for adaptive optimization of decomposition parameters, such as the number of modes and bandwidth, which enhances the accuracy but increases complexity.

In contrast, the LSTM and BNN models, which are based on the decomposed data, exhibit relatively low computational complexity. These models are implemented using MATLAB toolboxes or modifications thereof, resulting in faster processing times. The LSTM model leverages its ability to handle long-term dependencies in time series data efficiently, making it suitable for rapid prediction tasks. Similarly, BNNs provide robustness and uncertainty quantification without significantly increasing computational demands.

Consequently, the proposed methodology remains versatile and does not significantly increase the overall computational burden. By integrating AVMD as a pre-processing stage for data decomposition, the subsequent modeling based on decomposed data and the integration of results can meet the requirements for timeliness.

4. Conclusion

In response to the significant impact of noise and capacity regeneration on the RUL prediction of lithium-ion batteries, this paper proposes an innovative data-driven method. The main advantages of this method are as follows:

1) An AVMD algorithm is proposed, using the kernel estimation of mutual information and the gradient of relative energy density as constraints. This overcomes the issue of the traditional VMD method, where the decomposition effect is significantly influenced by the decomposition level and the balance parameter.
2) The PE method is used to filter out the aging trend sequences and capacity regeneration sequences, while removing the noise sequences that contain less effective information.
3) An LSTM model captures long-term dependencies in battery degradation, and BNNs express uncertainties due to capacity regeneration. The proposed method has significantly outperformed the standalone LSTM model, with the MAE, RMSE, and MAPE reduced by 63%, 54%, and 61%, respectively, demonstrating a clear superiority.

References

Bandt, C., & Pompe, B. (2002). Permutation Entropy: A Natural Complexity Measure for Time Series. *Physical Review Letters*, *88*(17).

Barré, A., Deguilhem, B., Grolleau, S., Gérard, M., Suard, F., & Riu, D. (2013). A review on lithium-ion battery ageing mechanisms and

estimations for automotive applications. In *Journal of Power Sources* (Vol. 241).

Cong, X., Zhang, C., Jiang, J., Zhang, W., & Jiang, Y. (2020). A Hybrid Method for the Prediction of the Remaining Useful Life of Lithium-Ion Batteries with Accelerated Capacity Degradation. *IEEE Transactions on Vehicular Technology*, *69*(11).

Ge, M. F., Liu, Y., Jiang, X., & Liu, J. (2021). A review on state of health estimations and remaining useful life prognostics of lithium-ion batteries. *Measurement: Journal of the International Measurement Confederation*, *174*.

Guha, A., Patra, A., & Vaisakh, K. V. (2017). Remaining useful life estimation of lithium-ion batteries based on the internal resistance growth model. *2017 Indian Control Conference, ICC 2017 - Proceedings*.

Jiang, X., Song, Q., Wang, H., Du, G., Guo, J., Shen, C., & Zhu, Z. (2022). Central frequency mode decomposition and its applications to the fault diagnosis of rotating machines. *Mechanism and Machine Theory*, *174*.

Jiang, X., Wang, J., Shi, J., Shen, C., Huang, W., & Zhu, Z. (2019). A coarse-to-fine decomposing strategy of VMD for extraction of weak repetitive transients in fault diagnosis of rotating machines. *Mechanical Systems and Signal Processing*, *116*.

Kumar, A., Zhou, Y., & Xiang, J. (2021). Optimization of VMD using kernel-based mutual information for the extraction of weak features to detect bearing defects. *Measurement: Journal of the International Measurement Confederation*, *168*.

Liu, J., Wang, W., Ma, F., Yang, Y. B., & Yang, C. S. (2012). A data-model-fusion prognostic framework for dynamic system state forecasting. *Engineering Applications of Artificial Intelligence*, *25*(4).

Liu, K., Shang, Y., Ouyang, Q., & Widanage, W. D. (2021). A Data-Driven Approach with Uncertainty Quantification for Predicting Future Capacities and Remaining Useful Life of Lithium-ion Battery. *IEEE Transactions on Industrial Electronics*, *68*(4).

Li, Y., Liu, K., Foley, A. M., Zülke, A., Berecibar, M., Nanini-Maury, E., Van Mierlo, J., & Hoster, H. E. (2019). Data-driven health estimation and lifetime prediction of lithium-ion batteries: A review. In *Renewable and Sustainable Energy Reviews* (Vol. 113).

Mirjalili, S. Z., Mirjalili, S., Saremi, S., Faris, H., & Aljarah, I. (2018). Grasshopper optimization algorithm for multi-objective optimization problems. *Applied Intelligence*, *48*(4).

Razavi-Far, R., Davilu, H., Palade, V., & Lucas, C. (2009). Model-based fault detection and isolation of a steam generator using neuro-fuzzy networks. *Neurocomputing*, *72*(13–15).

Richardson, R. R., Osborne, M. A., & Howey, D. A. (2017). Gaussian process regression for forecasting battery state of health. *Journal of Power Sources*, *357*. h

Song, K., Hu, D., Tong, Y., & Yue, X. (2023). Remaining life prediction of lithium-ion batteries based on health management: A review. In *Journal of Energy Storage* (Vol. 57).

Waag, W., Fleischer, C., & Sauer, D. U. (2014). Critical review of the methods for monitoring of lithium-ion batteries in electric and hybrid vehicles. In *Journal of Power Sources* (Vol. 258).

Wang, Y., Zhu, J., Cao, L., Gopaluni, B., & Cao, Y. (2023). Long Short-Term Memory Network with Transfer Learning for Lithium-ion Battery Capacity Fade and Cycle Life Prediction. *Applied Energy*, *350*.

Wu, J., Zhang, C., & Chen, Z. (2016). An online method for lithium-ion battery remaining useful life estimation using importance sampling and neural networks. *Applied Energy*, *173*.

Yang, X. G., Leng, Y., Zhang, G., Ge, S., & Wang, C. Y. (2017). Modeling of lithium plating induced aging of lithium-ion batteries: Transition from linear to nonlinear aging. *Journal of Power Sources*, *360*.

Zhang, C., He, Y., Yuan, L., & Xiang, S. (2017). Capacity Prognostics of Lithium-Ion Batteries using EMD Denoising and Multiple Kernel RVM. *IEEE Access*, *5*, 12061–12070.

Zhang, Y., Xiong, R., He, H., & Pecht, M. G. (2018). Long short-term memory recurrent neural network for remaining useful life prediction of lithium-ion batteries. *IEEE Transactions on Vehicular Technology*, *67*(7).